

# $J/\psi$ AND $\psi(2S)$ PRODUCTION IN SMALL SYSTEMS WITH PHENIX\*

KRISTA SMITH

on behalf of the PHENIX Collaboration

Los Alamos National Laboratory, USA

*Received 26 July 2022, accepted 30 August 2022,  
published online 14 December 2022*

The suppression of the  $\psi(2S)$  nuclear modification factor has been seen as a trademark signature of final-state effects in large collision systems for decades. In small systems, deviations of the nuclear modification from unity had been attributed to cold nuclear matter effects until the observation of strong differential suppression of the  $\psi(2S)$  state in  $p/d+A$  collisions, which suggests the presence of final-state effects. In this paper, we present results of  $J/\psi$  and  $\psi(2S)$  measurements in the dimuon decay channel for  $p+p$ ,  $p+Al$ , and  $p+Au$  collision systems at  $\sqrt{s_{NN}} = 200$  GeV. Key results include the nuclear modification factors  $R_{pA}$  as a function of centrality and rapidity. The measurements are compared with shadowing and transport model predictions, as well as complementary measurements at LHC energies.

DOI:10.5506/APhysPolBSupp.16.1-A73

## 1. Introduction

We present the first results of PHENIX  $\psi(2S)$  nuclear modification measurements at forward and backward rapidity. Here, we discuss a selected number of results from a recent PHENIX publication [1] that looked for signs of final-state effects on charmonium production in small system collisions at RHIC energies.

## 2. Experimental overview and data analysis

The PHENIX Muon Arms are located parallel to the beam pipe, and measure muons and unidentified charged hadrons at forward ( $1.2 < \eta < 2.4$ ) and backward ( $-2.2 < \eta < -1.2$ ) rapidity. The Muon Arms comprise four main components: the FVTX Detector, the Muon Tracker, the Muon

---

\* Presented at the 29<sup>th</sup> International Conference on Ultrarelativistic Nucleus–Nucleus Collisions: Quark Matter 2022, Kraków, Poland, 4–10 April, 2022.

Identifier, and a series of steel hadron absorbers located throughout each Muon Arm. The measurements were attainable using the Forward Vertex Silicon Detector (FVTX), installed in the PHENIX 2012 upgrade, which covers the pseudorapidity range  $1.2 < |\eta| < 2.2$ . The FVTX detector, a precision silicon tracking detector, provides additional space points closest to the interaction region, supplying the mass resolution necessary to extract the  $\psi(2S)$  signal.

The  $\psi(2S)$  measurements are presented in three small system data sets at the center-of-mass energy  $\sqrt{s_{NN}} = 200$  GeV:  $p+p$ ,  $p+Al$ , and  $p+Au$  collisions, all recorded during the 2015 run year. Measurements taken at forward rapidity denote the  $p$ -going direction of the collision, while backward rapidity denotes the Al/Au-going direction. In this analysis, the FVTX detector was used in conjunction with the Muon Tracker and the Muon Identifier to reconstruct the dimuon invariant mass. Previous PHENIX  $\psi(2S)$  measurements [2] required both tracks in the reconstructed dimuon pairs to be within the FVTX acceptance region. This requirement significantly improves the reconstructed dimuon mass resolution, but at the expense of statistics due to the limited geometric acceptance of the FVTX detector.

A new analysis method was developed to extract the  $\psi(2S)$  nuclear modification measurement in the PHENIX Muon Arms. This method combines muon tracks inside and outside the FVTX acceptance region, increasing the available statistics (see figure 1). Dimuon pairs are reconstructed in two different ways: both muon tracks are within the FVTX acceptance (denoted by Intersection B of figure 1) or just one muon track is inside the FVTX acceptance (denoted by Intersections A and C).

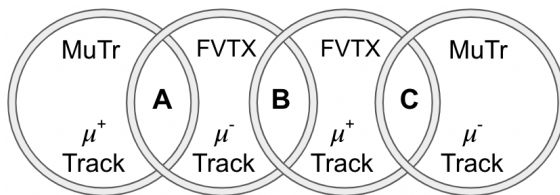


Fig. 1. Venn diagram illustrating the different combinations of reconstructed dimuon pairs used to increase the statistics available for the  $\psi(2S)$  measurements while still utilizing the mass resolution of the FVTX detector.

### 3. Results

Shown in figure 2 is the  $\psi(2S)$  (open black data points) and  $J/\psi$  (solid black) nuclear modification factor in  $p+Al$  collisions. The measurements correspond to  $p_T > 0$  GeV/ $c$  and are taken over the full rapidity range of  $1.2 < |y| < 2.2$ . At forward rapidity, the nuclear modification measurements

are consistent between the two states. There is little to no nuclear modification, as would be expected from a lighter aluminum target. As observed in a similar PHENIX analysis [3],  $J/\psi$  nuclear modification measurements did not show any effects of gluon shadowing at forward rapidity.

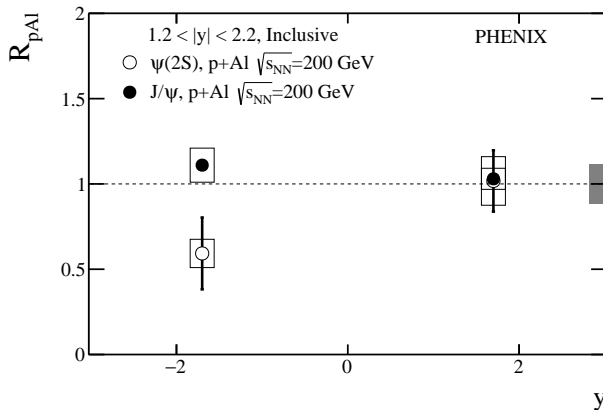


Fig. 2. The  $p_T$  and centrality-integrated nuclear modification factors as a function of rapidity for  $\psi(2S)$  [open circles] and  $J/\psi$  [solid circles] in  $p$ +Al collisions.

At backward rapidity, the  $J/\psi$  nuclear modification measurement is consistent with unity. This implies that gluon anti-shadowing and nuclear absorption effects, if any, are small. Therefore, the suppression seen in the  $\psi(2S)$  nuclear modification factor at backward rapidity cannot be attributed to nuclear absorption. This suppression is possibly due to final-state effects, but the error bars are large and do not permit a clear conclusion.

A complementary measurement in the  $p$ +Au collision system is shown in figure 3. The  $\psi(2S)$  nuclear modification measurements (red squares) are compared with the  $J/\psi$  nuclear modification measurements (black circles). Again, the modification between the two states is consistent at forward rapidity. The data is well described by EPPS16 [4] and nCTEQ15 [5] re-weighted gluon shadowing predictions [6] as the source of suppression at forward rapidity.

At backward rapidity, the  $J/\psi$  suppression can be understood as a trade-off between the competing effects of anti-shadowing and nuclear absorption. Cold nuclear matter effects for the  $J/\psi$  and  $\psi(2S)$  states are expected to be similar for measurements recorded with the same rapidity, collision system, and collision energy. Therefore, nuclear absorption cannot explain the suppression of the  $\psi(2S)$  nuclear modification with respect to the  $J/\psi$  suppression. Furthermore, gluon shadowing alone cannot describe the data.

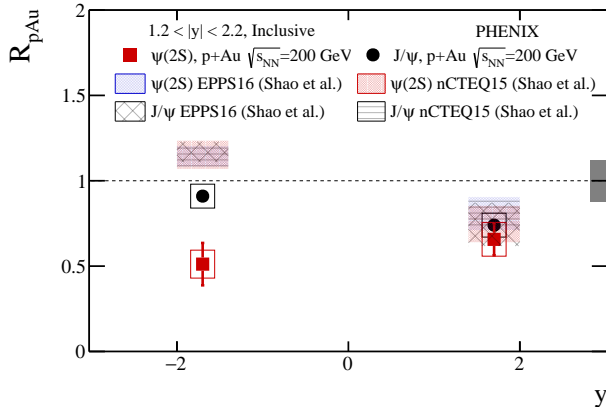


Fig. 3. (Color online) The  $p_T$  and centrality-integrated nuclear modification factors as a function of rapidity for  $\psi(2S)$  [red squares] and  $J/\psi$  [black circles] in  $p+Au$  collisions. The data are compared to EPPS16 and nCTEQ15 shadowing predictions.

Figure 4 shows the  $\psi(2S)$ -to- $J/\psi$  ratio as a function of  $\langle N_{\text{coll}} \rangle$ . The PHENIX data in  $p+Au$  collisions (solid red squares) are directly compared to ALICE data [7] in  $p+Pb$  collisions (solid black circles). The corresponding  $\psi(2S)$ -to- $J/\psi$  ratio by PHENIX (open red square) and ALICE (open black circle) is shown for  $p+p$  collisions at  $\langle N_{\text{coll}} \rangle = 1$ . Previous publications [2] have shown that the  $\psi(2S)$ -to- $J/\psi$  ratio in  $p+p$  collisions is independent of collision energy. It is expected that by taking the ratio of the two charmonium states, cold nuclear matter effects largely cancel, leaving final-state effects as the dominant contribution. Despite the different Bjorken- $x$  and  $Q^2$

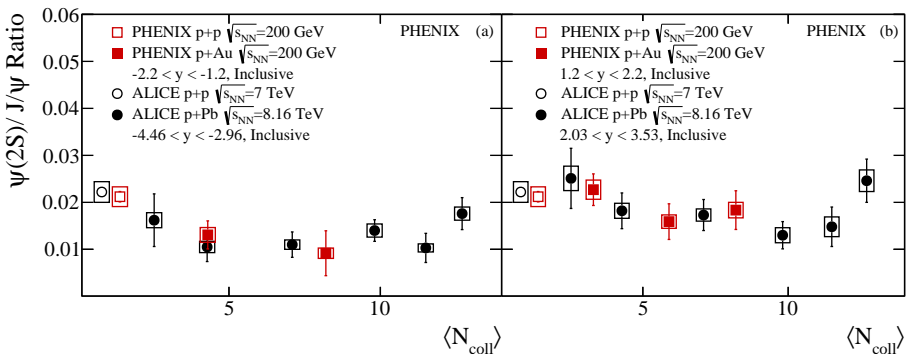


Fig. 4. (Color online) The  $\psi(2S)$ -to- $J/\psi$  ratio is shown as a function of  $\langle N_{\text{coll}} \rangle$  at backward (a) and forward (b) rapidity. PHENIX data in  $p+Au$  collisions compared to ALICE data in  $p+Pb$  collisions. The corresponding ratios in  $p+p$  collisions for each experiment are shown for  $\langle N_{\text{coll}} \rangle = 1$ .

regions probed by the two experiments, the ratio as a function of centrality is quite similar, particularly at backward rapidity. It is worth noting that the Lorentz factor is larger at LHC energies, which might allow charmonium to escape the interaction region more quickly than at RHIC energies.

Lastly, a more comprehensive comparison of charmonium nuclear modification measurements is shown at both RHIC and LHC energies in figure 5. The  $J/\psi$  ( $\psi(2S)$ ) nuclear modification is denoted with the open (solid) data points. The measurements are taken over a variety of small collision systems, including RHIC  $p$ +Au and  $d$ +Au collisions at  $\sqrt{s_{NN}} = 200$  GeV, and LHC  $p$ +Pb collisions at  $\sqrt{s_{NN}} = 5$  TeV. The current PHENIX  $p$ +Au results are shown in blue, previous PHENIX  $d$ +Au measurements in gold [8], and LHCb [9, 10] and ALICE [11, 12] in red and gray, respectively. At forward rapidity, similar modification is seen between  $J/\psi$  and  $\psi(2S)$ , indicating cold nuclear matter effects are dominant. At backward rapidity, stronger  $\psi(2S)$  suppression is seen across all three experiments, strongly suggesting that final-state effects are present in small collision systems.

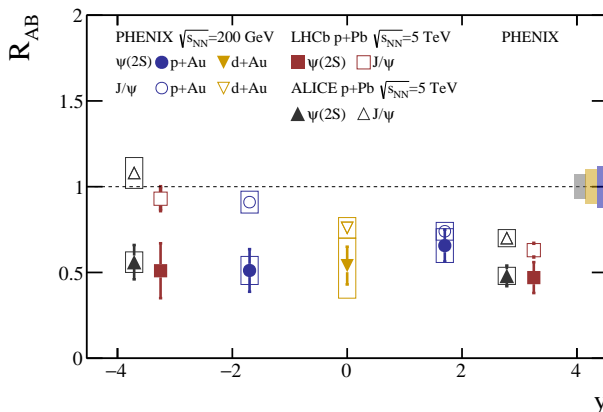


Fig. 5. (Color online) Nuclear modification measurements for  $\psi(2S)$  (solid data points) and  $J/\psi$  (open data points) are shown for the PHENIX, LHCb, and ALICE experiments as a function of rapidity by the blue circles, red squares, and gray triangles, respectively. Refer to the text for more details.

#### 4. Conclusion

We have presented  $p_T$ -integrated charmonium nuclear modification measurements and the  $\psi(2S)$ -to- $J/\psi$  ratio as a function of centrality at forward and backward rapidity, and compared PHENIX measurements with those taken at LHCb and ALICE. The data suggest that gluon shadowing is the dominant contribution to modification at forward rapidity for both the

$J/\psi$  and the  $\psi(2S)$  states. At backward rapidity, we find stronger suppression of the  $\psi(2S)$  with respect to the  $J/\psi$ , a signature historically attributed to color screening. Additionally, the  $\psi(2S)$ -to- $J/\psi$  ratio is surprisingly similar between PHENIX and ALICE data, particularly at backward rapidity, suggesting that final-state effects are similar at RHIC and LHC energies.

## REFERENCES

- [1] PHENIX Collaboration (U.A. Acharya *et al.*), *Phys. Rev. C* **105**, 064912 (2022).
- [2] PHENIX Collaboration (A. Adare *et al.*), *Phys. Rev. C* **95**, 034904 (2017).
- [3] PHENIX Collaboration (U. Acharya *et al.*), *Phys. Rev. C* **102**, 014902 (2020), [arXiv:1910.14487 \[hep-ex\]](https://arxiv.org/abs/1910.14487).
- [4] K.J. Eskola, P. Paakkinen, H. Paukkunen, C.A. Salgado, *Eur. Phys. J. C* **77**, 163 (2017).
- [5] K. Kovarik *et al.*, *Phys. Rev. D* **93**, 085037 (2016).
- [6] A. Kusina, J.-P. Lansberg, I. Schienbein, H.-S. Shao, *Phys. Rev. Lett.* **121**, 052004 (2018).
- [7] ALICE Collaboration (S. Acharya *et al.*), *J. High Energy Phys.* **2021**, 002 (2021).
- [8] PHENIX Collaboration (A. Adare *et al.*), *Phys. Rev. Lett.* **111**, 202301 (2013).
- [9] LHCb Collaboration (R. Aaij *et al.*), *J. High Energy Phys.* **2016**, 133 (2016).
- [10] LHCb Collaboration (R. Aaij *et al.*), *J. High Energy Phys.* **1402**, 072 (2014).
- [11] ALICE Collaboration (B.B. Abelev *et al.*), *J. High Energy Phys.* **1024**, 73 (2014).
- [12] ALICE Collaboration (B.B. Abelev *et al.*), *J. High Energy Phys.* **1412**, 73 (2014).